Smart Structures and Systems, *Vol. 23, No. 5 (2019) 421-428*
DOI: https://doi.org/10.12989/sss.2019.23.5.421

Dynamic analysis and performance optimization of permendur cantilevered energy harvester

Mojtaba Ghodsi*[1], Hamidreza Ziaiefar[1], Morteza Mohammadzaheri[1], Farag K. Omar[2] and Issam Bahadur[1]

[1]Mechanical and Industrial Engineering Department, College of Engineering , Sultan Qaboos University, Muscat, Oman
[2] Mechanical Engineering Department, College of Engineering, United Arab Emirates University, AlAin, UAE

(Received September 16, 2018, Revised April 1, 2019, Accepted April 8, 2019)

Abstract. The development of the low power application such as wireless sensors and health monitoring systems, attract a great attention to low power vibration energy harvesters. The recent vibration energy harvesters use smart materials in their structures to convert ambient mechanical energy into electricity. The frequent model of this harvesters is cantilevered beam. In the literature, the base excitation cantilevered harvesters are mainly investigated, and the related models are presented. This paper investigates a tip excitation cantilevered beam energy harvester with permendur. In the first section, the mechanical model of the harvester and magneto-mechanical model of the permendur are presented. Later, to find the maximum output of the harvester, based on the response surface method (RSM), some experiments are done, and the results are analyzed. Finally, to verify the results of RSM, a harvester with optimum design variables is made, and its output power is compared. The last comparison verifies the estimation of the RSM method which was about 381 $\mu W/cm^3$.

Keywords: vibration energy harvesting; tip excitation; mechanical model; smart material; performance optimization; permendur; RSM method

1. Introduction

The attention to energy harvesters has been increased during the past years. Harvesters can be implemented in many autonomous systems such as health monitoring systems, wireless sensors, medical implants, etc. The advancement in the production of low power ICs such as ADXL372 (micropower 3-axis accelerometer) or ADS7866 (low power data acquisition IC) and development of more efficient energy harvesters have made it possible to have an independent battery-less wireless application. Energy harvesters can convert the ambient wasted energy to a useful energy like electricity. Due to several sources of ambient energy, from the sunlight to the wave movements in oceans, there are various types of energy harvesters. One of the main sources for harvesting energy is the kinetic energy of vibration. Vibration can be seen almost everywhere. From natural movements of a muscle in the human body to the vibration of the drilling machine in a car, factory can be used as to light up LED (Xia *et al.* 2019). A suitable energy harvester can use this vibration to generate enough electricity to run a low power application. One of the most common designs of vibration energy harvesters is based on the magnetostrictive material (MSM). MSM is a kind of smart material that can convert kinetic energy to magnetic energy and vice versa. This ability makes it a suitable choice for using in many applications such as harvesters (Fang *et al.* 2017, Li *et al.* 2017, Ghodsi *et al.* 2018, Li *et al.* 2018), sensors (Ghodsi *et al.* 2015), and actuators(Ghodsi *et al.* 2007, Ghodsi *et al*. 2008, Ghodsi *et al.* 2011, Karafi *et al.* 2013, Karafi *et al.* 2015, Sheykholeslami *et al.* 2015, Sheykholeslami *et al.* 2016, Ghodsi *et al.* 2017). Cantilevered beam harvesters are one the most common mechanisms to use MSM for conversion. A cantilevered beam energy harvester is a fixed-free beam with an MSM bar or plate (Fig. 1). During operation, the beam is under an external force of vibration and accordingly, the MSM is under repetitive tension and compression bending-stress. According to Villari effect, the mechanical stress changes the magnetization of the MSM. Due to this effect, by using a pick-up coil around the MSM, based on Faraday’s law, a voltage will be induced in it.

There are many types of research on energy harvesters. Some scientists have focused on the design of the micro or macro scale harvesters (Kumar *et al.* 2015, Zhang *et al.* 2018). The other group has worked on the related electrical circuit for voltage and current regulation for providing to the consumer device (Lefeuvre *et al.* 2007). The third group has investigated the optimization of the individual parts of energy harvesters.

In this research permendur 2V (an Iron-Cobalt alloy with two percent of Vanadium) is used as the energy converter. Permendur is a soft alloy and in comparison to PZTs (the most common energy converter material in harvesters (Hoshyarmanesh *et al.* 2014) has higher Young's modulus, higher relative magnetic permeability, and machinability. Permendur is not brittle and can be used in a harsh working condition with mechanical shocks.

*Corresponding author, Dr.
E-mail: ghodsi@squ.edu.om

http://www.techno-press.com/journals/sss&subpage=7
ISSN: 1738-1584 (Print), 1738-1991 (Online)

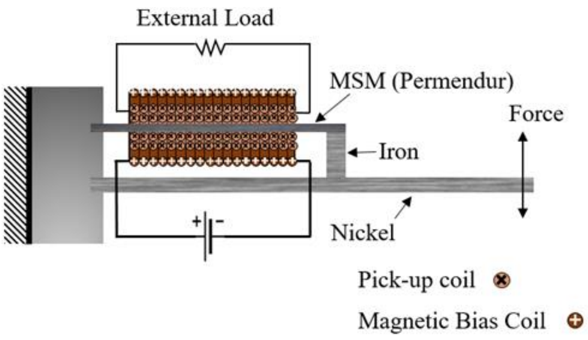

Fig. 1 Schematic view of the MSM cantilevered harvester

In contrast to PZT, permendur needs magnetic bias to have maximum performance. Magnetic DC bias shifts the operating condition from non-linear region to linear region in the B-H curve and enhance the magnetic permeability of permendur. The exact value of the magnetic bias field is varied for each material. Without having the optimal value of magnetic bias, the permendur does not show the best efficiency.

The objective of this article is to find the optimum parameters in the design of a cantilevered permendur energy harvester for work under a specific vibration force condition.

The output parameter is the measured power. Based on the initial investigation, the design parameters are external load resistance, magnetic bias and number of turns in pick-up coil. The presented approach studies all design trade-offs of a cantilevered energy harvester.

This article has two main sections. In the first section, the mechanical solution for the displacement of the cantilevered harvester with the fixed base under harmonic excitation is derived. In the second section, some experiments are done, and the maximum output performance of the harvester and its related variables are found.

2. Dynamic analysis

The cantilever energy harvester can be considered as a clamped-free beam. At one end, the beam is fixed and has no displacement or rotation. At the other end, the beam is free. For this harvester, the external force is a transverse harmonic excitation that can be applied at any point of the beam. Using Euler-Bernoulli equation, the absolute displacement of the beam at each point can be written in the form of Eq. (1).

$$EI\frac{\partial^4 \nu(x,t)}{\partial x^4}+\mu\frac{\partial^2 \mathrm{v}(\mathrm{x},\mathrm{t})}{\partial t^2}=p(x,t) \tag{1}$$

In Eq. (1), $\nu(x,t)$ is the displacement of the point x at time t. E is Young's modulus, I is the moment of inertia of the cross section and *p(x,t)* is the applied force to the beam. In this equation, the force can be applied at any point of the beam. The applied oscillating force to the harvester is considered harmonic. Hence, the force can be modeled as

$$p(x,t)=F_0\,\mathrm{e}^{j\omega t}\delta\big(x-x_f\big) \tag{2}$$

where F_0 is the amplitude of the oscillating force, ω and x_f is the frequency and position of the applied force and j is the imaginary unit or $\sqrt{-1}$.

By substituting Eq. (2) in Eq. (1), the displacement of the beam can be written as

$$EI\frac{\partial^4 \mathrm{v}(x,t)}{\partial x^4}+\mu\frac{\partial^2 \mathrm{v}(\mathrm{x},\mathrm{t})}{\partial t^2}=F_0\,\mathrm{e}^{j\omega t}\delta\big(x-x_f\big) \tag{3}$$

Eq. (3) is a partial differential equation, and the solution can be assumed as

$$EI\frac{\partial^4 \nu(x,t)}{\partial x^4}+\mu\frac{\partial^2 \mathrm{v}(\mathrm{x},\mathrm{t})}{\partial t^2}=p(x,t) \tag{4}$$

Solving this partial differential equation needs the boundary conditions. For this harvester, the cantilevered beam is fixed in one end (*x=0*), so the displacement and derivation of the displacement are zero at this end. At the other end of the beam (*x=L*), the beam is free, and there is no bending moment and shearing force at this end. Hence, the four boundary conditions can be written as

$$x=0\rightarrow\begin{cases}X(0)=0\\X'(0)=0\end{cases} \tag{5}$$

$$x=L\rightarrow\begin{cases}X''(L)=0\\X'''(L)=0\end{cases} \tag{6}$$

Different solution can be implemented to solve Eq. (3). In this paper, by considering the boundary condition and using Laplace transform and Green function, Eq. (3) is solved as

$$\begin{aligned}X(x)=\frac{1}{2k^3EI}\int_0^L &(\sinh\ k\big(x-x_f\big)\\&-\sin k\big(x-x_f\big))\,u\big(x-x_f\big)\\&+M_1\Big((\sinh\ k\big(x-x_f\big)\\&-\sin k\big(x-x_f\big))\,u\big(x-x_f\big)\Big)\\&+M_2((\cosh\ k\big(x-x_f\big)\\&+\cos k\big(x-x_f\big))f\big(x_f\big)\,dx_f\end{aligned} \tag{7}$$

where $u(x)$ is the unit step function and k, M_1 and M_2 are (Eq. (8))

$$k = \sqrt[4]{\frac{\mu\omega^2}{EI}}$$
$$M_1 = \frac{(\sinh kL - \sin kL)\,(\sinh k(L - x_f) + \sin(L - x_f)) - (\cosh kL + \cos L)(\cosh k(L - x_f) + \cos k(L - x_f))}{(\cosh kL + \cos L)^2 - (\sinh kL + \sin kL)(\sinh kL - \sin kL)} \tag{8}$$
$$M_2 = \frac{(\sinh kL + \sin kL)\,(\cosh k(L - x_f) + \cos(L - x_f)) - (\cosh kL + \cos L)(\sinh k(L - x_f) + \sin k(L - x_f))}{(\cosh kL + \cos L)^2 - (\sinh kL + \sin kL)(\sinh kL - \sin kL)}$$

Substituting this equation into Eq. (4) gives us the displacement of the beam in each point under a harmonic force.

At this point, by finding the mechanical response of the harvester under harmonic force, the magneto-mechanical model can be solved, and the output performance can be found. Magneto-mechanical model gives the output power of the harvester based on the strain of MSM at each point. The magneto-mechanical behavior of permendur in a cantilevered energy harvester with different external load has already been investigated by authors (Ghodsi *et al.* 2018). Therefore, to avoid repeating, this equations and the solution are not provided here.

3. Experimental setup

For the experiment, a 90 mm length cantilevered beam harvester with a permendur plate is fabricated. The harvester uses a 40×7×1 mm^3 permendur plate with surrounded by two separate coil. One coil is pick-up coil responsible for generating electricity and the second coil is bias magnetic coil responsible for generating a constant magnetic field. Fig. 3 shows the setup of the experiment.

To measure the output of the harvester, an analog to the digital card (ADC) is implemented. The ADC model is CompuScope 14100 with 14 Bit resolution and 100 MS/s sampling rate. For measuring the displacement of the beam at the free end, a displacement sensor, model HK052, is implemented.

Based on the mechanical, the harvester excitation frequency is set at 130 Hz which is equal to its natural frequency. Moreover, based on magneto-mechanical model, important variables of the harvester are found. To find the maximum possible output in a real condition and via experiment, all of the variables have to be tested. In this condition, it is beneficial to use a design of experiment method to find the maximum output with a minimum number of experiments.

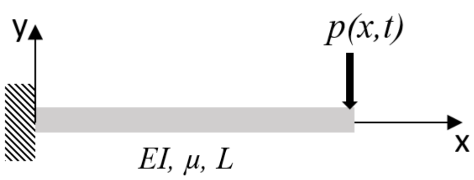

Fig. 2 Schematic of a cantilevered beam

The factors for optimization process are from both harvester and consumer. For the consumer, it is obvious that each circuit has a specific electrical characteristic such as resistance, capacitance, and inductance. Each of these properties can have a different impact on the generated voltage and power of the harvester. On the other hand, in many electrical circuits, the impact of one factor is dominant, and the other factors can be neglected with an acceptable error. Considering all the above points, to simplify the experiment, the external electrical consumer is assumed as a purely resistive load.

Moreover, according to (Ghodsi *et al.* 2018) the bias magnetic field and the number of turns in the pick- up coil also can have a significant impact on the overall performance. Therefore, at last, three factors (load resistance, number of turns in pick-up coil and bias magnetic field) are used as some independent input variables. To manifest the interactions of factors in the harvester, design, and analysis of the experiment (DOE) is employed. Additionally, to optimize the generated power and selected the proper nominal values for each factor, Response Surface Method (RSM) is utilized. RSM is a combination of statistical and mathematical methods that is a suitable technique for optimization of nonlinear systems (Aloufi and Kazmierski 2011, Ghodsi 2015).

Fig. 3 The experimental setup

Table 1 Input variables

Factors	Unit	- α	Low (-1)	Center (0)	High (+1)	+ α
R: Load Resistance	Ω	0.1	2.8	5.5	8.3	11.1
N: Number Of Turns In Pick-Up Coil	-	80	160	240	320	400
H: Bias Magnetic Field	kA/m	0	3.3	6.6	9.9	13.2

Table 2 Experiment Results Based on the RSM

Run Order	R	N	H	Voltage (mV)	Power (μW)
1	0	2	0	20.00	74.07
2	1	1	-1	6.50	5.21
3	1	-1	1	11.00	14.94
4	0	0	0	14.00	36.30
5	0	0	0	13.75	35.01
6	0	0	0	14.25	37.60
7	0	0	0	14.00	36.30
8	-1	1	1	14.50	77.87
9	-1	-1	-1	2.60	2.50
10	0	-2	0	3.25	1.95
11	0	0	0	14.00	36.30
12	1	1	1	19.50	46.94
13	-1	1	-1	4.00	5.92
14	-1	-1	1	7.80	22.53
15	1	-1	-1	3.05	1.15
16	-2	0	0	1.25	8.22
17	0	0	-2	0.75	0.10
18	2	0	0	16.00	23.70
19	0	0	2	8.50	31.30
20	0	0	0	14.50	38.93
21	1	1	-2	2.00	0.12
22	0	1	2	12.00	26.66

The first step in the design of an experiment using RSM is the finding the mathematical model. To find the correlation between responses and variables, central composite design (CCD) is used and the model is found in Minitab 17. Table 1 shows the input variables with five level by considering $\alpha=2$. The minimum and maximum values for each factor are estimated based on the previous experiments.

The generated power and voltage with different variables are shown in Table 2. In the table, the variables are shown in coded values. To minimize the uncontrolled variables, in the CCD step, the experiments have been done randomly. As presented in Table 2, three independent variables are load resistance (R), some turns in pick-up coil (N) and bias magnetic field (H).

Measured voltage of two experiments are shown in the Fig. 4. It is required to add that the output voltage is the voltage across the external resistive load (Fig. 1). When the load is small, the drop voltage across load is small (e.g., in short circuit condition the output voltage is zero). By increasing the external resistive load, the output voltage (drop voltage across the external load) becomes larger. Consequently, the output voltage saturates when it is open circuit. Although voltage culminates by increasing resistive load, the power is inversely proportional to the external resistance load. Therefore, the power will reach to its maximum value in one specific resistance and mitigates in higher value of resistance (Fig. 5).

Table 3 shows the analysis of variables for CCD. To obtain the interaction among the responses and variables, the data are evaluated including analysis of variance (ANOVA). Moreover, to check the quality of the model, the correlation coefficient and the F-test was used to check the statistical significance. Regarding the coefficient in Table 3, the generated power of the harvester can be modeled as

$$
\begin{aligned}
Power = 36.83 &- 0.33\,R + 13.93\,N + 9.99\,H \\
&- 5.38\,R^2 - 0.51\,N^2 - 7.61\,H^2 \\
&- 2.28\,R \times N - 5.66\,R \times H \\
&+ 3.73\,N \times H - 5.66\,R * H \\
&+ 3.73\,N * H
\end{aligned} \tag{9}
$$

and *R-Sq* is 79.5%, and *R-Sq(adj)* is 64.24%.

It should be mentioned that in analyzing the results, with 95% reliability, factors with the P_{value} lower than 0.05 are effective. Fig. 5 shows the effect of each parameter on the generated power of the harvester.

Fig. 6 to Fig. 8 show the interaction between variables and generated power.

A. Influence of external load resistance

The results show that although the resistance of the external load has an impact on the generated power of the harvester, in comparison to *H* and *N*, its impact is insignificant.

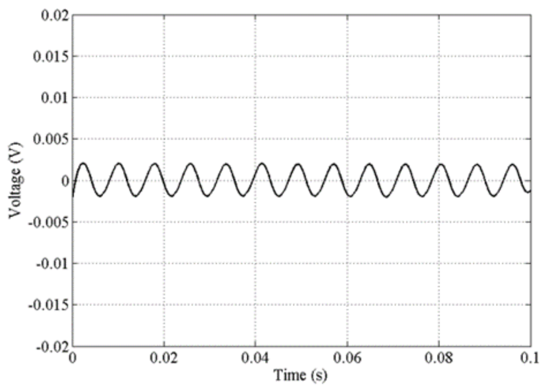

(a) R= -1, N= -1, H= -1

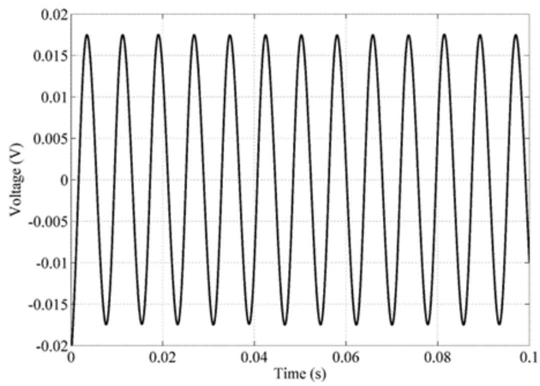

(b) R= +1, N= +1, H= +1

Fig. 4 Generated voltage of the harvester

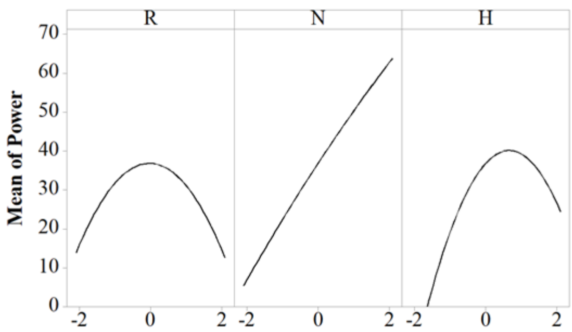

Fig. 5 The Effects of each parameter on the generated power

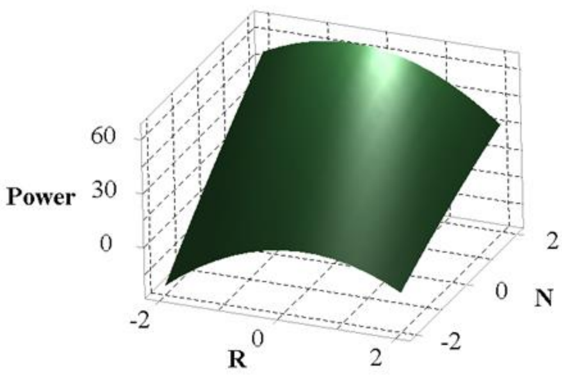

Fig. 6 Interaction of the coded resistance and number of turns in pick-up coil on power

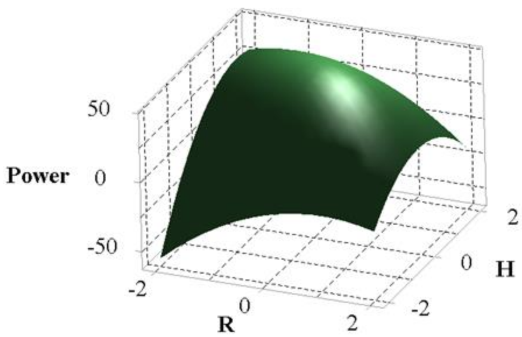

Fig. 7 Interaction of the coded resistance and bias magnetic field on power

By increasing the load resistance, the generated voltage will increase continuously to reach its maximum value, but according to $= \frac{V^2}{R}$, the power shows a different trend. Therefore, it can be said that the performance of the harvester is not related to the resistance of the external load (purely resistive load).

Table 3 Analysis of variance for CCD

Terms	Sum Of Square	Degree Of Freedom	Mean Square	F-Value	P-Value
R	1.7	1	1.74	0.01	0.923
N	3280.2	1	3280.2	18.26	0.001
H	1942.9	1	1942.89	10.82	0.006
R2	735.9	1	735.9	4.10	0.066
N2	6.7	1	6.69	0.04	0.850
H2	2209.5	1	2209.52	12.30	0.004
R×N	43.6	1	43.59	43.59	0.631
R×H	308.4	1	308.37	3.8.37	0.215
N×H	172.7	1	172.71	172.71	0.346
Lack of Fit	2146.0	7	306.56	306.56	
Pure Error	9	5	1.83	1.83	
Total	10545	21			

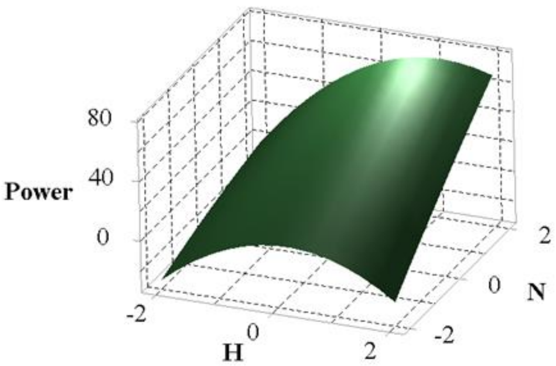

Fig. 8 Interaction of the coded number of turns in pick-up coil and bias magnetic field on power

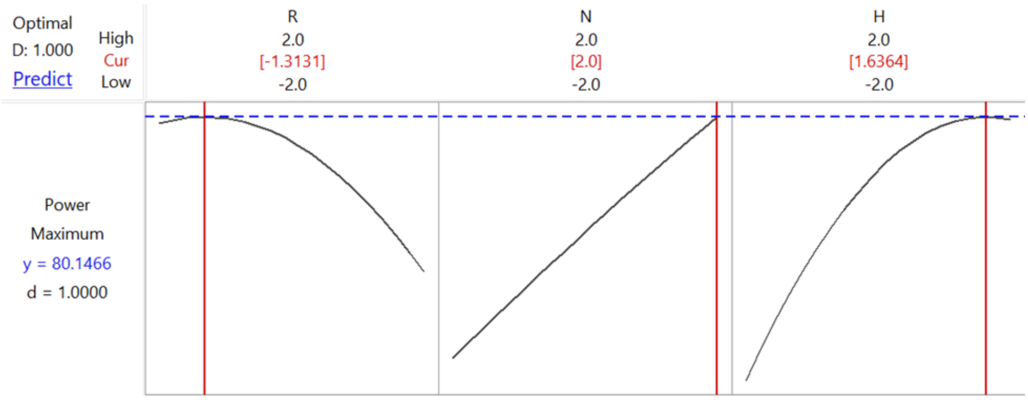

Fig. 9 The optimum values to have maximum generated power

B. Influence of magnetic DC bias

The influence of the bias magnetic field is intense. The optimization plot shows that the system has the maximum output at 12 *kA/m* magnetic field. This phenomenon can be explained by two reasons. First of all, the magnetic bias changes the shape of magnetic domains in the permendur. According to the datasheet of the tested permendur, this material will be saturated at magnetic fields over 12 *kA/m* which is completely equal to the results of the experiment. That means by using the permendur in the saturated condition; the performance will decrease significantly.

Moreover, based on Sheykholeslami article on the effect of magnetic field on mechanical properties of permendur (Sheykholeslami *et al.* 2016), the lowest Young modulus of permendur can be seen near the saturation point. In this situation, with a constant force of wasted vibration,

the harvester has more flexibility and a higher rate of displacement when the permendur has lower Young modulus. However, it should be considered that the first factor is more dominant.

C. Number of turns in the pick-up coil

It is obvious that by increasing the number of turns in the pickup coil, the generated voltage and power of the harvester will increase. In this research, the increase in the number of turns from 80 to 400 increases the generated voltage and power. However, it should be mentioned that a pick-up coil with a higher number of turns has higher size and mass which is a limitation of many designs like MEMS.

4. Optimization

By finding the model of generated power in the harvester, the influence of each factor and the optimum values can be found easily. Fig. 9 shows the prediction of the RSM to have the maximum generated power. According to this figure, a harvester with $R= -1.31$, $N=+2$ and $H=1.63$ generates the most possible power. These coded values and the related real values of each parameter are indicated in Table 4. To verify the RSM mode, a new harvester is fabricated and tested. As it can be seen in the table, the predicted value of the power and the measured power from the experiment are very close and is the maximum measured power in all of the experiments.

5. Conclusions

Cantilevered energy harvesters are one of the most common designs of vibration harvesters and have been subjected to many articles. Generally, these harvesters have base excitation. In this study, a permendur cantilevered energy harvester is designed, fabricated and tested. To analyze the dynamic performance of the harvester, the general solution of a cantilevered beam harvester with a fixed base is derived. In the solution, the Euler-Bernoulli beam is considered, and the external transverse force is applied to the free end of the beam. Later, by finding important variables of the harvester, few harvesters are fabricated, and some tests are done. To find the best possible variable in the design of the harvester with a minimum number of experiments, RSM method is implemented. Using RSM, the design variables of the harvester such as external load resistance, the number of turns in the pickup coil and bias magnetic field are optimized, and the impact of each factor on the generated power is discussed. In the end, a harvester with the optimum values is fabricated, and the results of the experiments and predicted power of the RSM are compared. The comparison shows that the harvester can generate about $381\ \mu W/cm^3$ electricity in its maximum performance.

Acknowledgments

This work was done under the project number (CL/SQU-UAEU/16/05) which was funded from the joint research project at Sultan Qaboos University in Oman.

References

Aloufi, M. and Kazmierski, T.J. (2011), “A response surface modelling approach to performance optimisation of kinetic energy harvesters”, *Int. J. Res. Rev. Comput.Sci.*: 1.

Fang, Z.W., Zhang, Y.W., Li, X., Ding, H. and Chen, L.Q. (2017), “Integration of a nonlinear energy sink and a giant magnetostrictive energy harvester”, *J. Sound Vib*., **391**, 35-49. https://doi.org/10.1016/j.jsv.2016.12.019

Ghodsi, M. (2015), “Optimization of mover acceleration in DC tubular linear direct-drive machine using response surface method”, *Int. Rev. Elec. Eng*., **10**(4), 492-500.

Ghodsi, M., Ueno, T. and Higuchi, T. (2008), “Novel .magnetostrictive bimetal actuator using permendur”, *Adv. Mater. Res.*, **47-50**, 262-265. https://doi.org/10.4028/www.scientific.net/AMR.47-50.262.

Ghodsi, M., Modabberifar, M. and Ueno, T. (2011), “Quality factor, static and dynamic responses of miniature galfenol actuator at wide range of temperature”, *Int. J. Phys. Sci.*, **6**(36): 8143-8150. DOI: 10.5897/IJPS11.918.

Ghodsi, M., Ueno, T., Teshima, H., Hirano, H., Higuchi, T. and Summers, E. (2007), “'Zero-power' positioning actuator for cryogenic environments by combining magnetostrictive bimetal and HTS”, *Sensor. Actuat. A: Phys*., **135**(2), 787-791. https://doi.org/10.1016/j.sna.2006.09.002.

Ghodsi, M., Ziaiefar, H., Alam, K., Mohammadzaheri, M., Al-Yahmedi, A. and Omar, F.K. (2018), “Electromechanical modelling and experimental verification of cantilevered permendur energy harvester”, *Proceedings of the IEEE/ASME International Conference on Advanced Intelligent Mechatronics*.

Ghodsi, M., Mirzamohamadi, S., Talebian, S., Hojjat, Y., Sheikhi, M., Al-Yahmedi, A. and Ö zer, A. (2015), “Analytical, numerical and experimental investigation of a giant magnetostrictive (GM) force sensor”, *Sensor Review*, **35**(4), 357-365. https://doi.org/10.1108/SR-12-2014-0760.

Ghodsi, M., Ziaiefar, H., Alam, K., Mohammadzahcri, M., Al-Yahmedi, A., Ghodsi, M.H. and Omar, F.K. (2018), “Electromechanical modelling and experimental verification of cantilevered permendur energy harvester”, *Proceedings of the 2018 IEEE/ASME International Conference on Advanced Intelligent Mechatronics (AIM), IEEE*.

Ghodsi, M., Hosseinzadeh, N., Ozer, A., H.R,. Dizaj, Y., Hojjat, Y., Varzeghani, N.G., Sheykholeslami, M.R., Talebian, S., Ghodsi M.H. and Al-Yahmadi, A. (2017), “Development of gasoline direct injector using giant magnetostrictive materials”, *IEEE T. Ind. Appl*., **53**(1), 521-529. DOI: 10.1109/TIA.2016.2606591.

Hoshyarmanesh, H., Nehzat, N., Salehi, M., Ghodsi, M., Lee, H.S. and Park, H.H. (2014), “Piezoelectric transducers on curved dispersive bending wave and poke-charged touch screens”, *Mater. Manuf. Process*., **29**(7), 870-876. https://doi.org/10.1080/10426914.2014.921710.

Karafi, M.R., Ghodsi, M. and Hojjat, Y. (2015), “Development of magnetostrictive resonant torsional vibrator”, *IEEE T. Magnetics*, **51**(9), 1-8. DOI: 10.1109/TMAG.2015.2427279.

Karafi, M.R., Hojjat, Y., Sassani, F. and Ghodsi, M. (2013), “A novel magnetostrictive torsional resonant transducer”, *Sensor. Actuat. A: Phys*., **195**, 71-78. https://doi.org/10.1016/j.sna.2013.03.015.

Kumar, T., Kumar, R., Chauhan, V.S. and Twiefel, J. (2015), "Finite-element analysis of a varying-width bistable piezoelectric energy harvester", *Energy Technol.*, **3**(12): 1243-1249. https://doi.org/10.1002/ente.201500191.

Lefeuvre, E., Audigier, D., Richard, C. and Guyomar, D. (2007), "Buck-boost converter for sensorless power optimization of piezoelectric energy harvester", *IEEE T. Power Electr.*, **22**(5), 2018-2025.

Li, X., Zhang, Y., Ding, H. and Chen, L. (2017), "Integration of a nonlinear energy sink and a piezoelectric energy harvester", *Appl. Math. Mech*., **38**(7), 1019-1030.

Li, X., Zhang, Y.W. Ding, H. and Chen, L.Q. (2018), "Dynamics and evaluation of a nonlinear energy sink integrated by a piezoelectric energy harvester under a harmonic excitation", *J. Vib. Control*, https://doi.org/10.1177/1077546318802456.

Sheykholeslami, M., Hojjat, Y., Ghodsi, M., Kakavand, K. and Cinquemani, S. (2015), "Investigation of ΔE effect on vibrational behavior of giant magnetostrictive transducers", J. *Shock Vib*., **2015**, 1-9. http://dx.doi.org/10.1155/2015/478045

Sheykholeslami, M., Hojjat, Y., Ghodsi, M., Zeighami, M. and Kakavand, K. (2016), "Effect of magnetic field on mechanical properties in Permendur", *Mater. Sci. Eng., A* **651**, 598-603. https://doi.org/10.1016/j.msea.2015.10.027.

Sheykholeslami, M.R., Hojjat, Y., Cinquemani, S., Ghodsi, M. and Karafi, M. (2016), "An approach to design and fabrication of resonant giant magnetostrictive transducer", *Smart Struct. Syst*.,**17**(2), 313-325. https://doi.org/10.12989/sss.2016.17.2.313.

Xia, M., Luo, C., Su, X., Li, Y., Li, P., Hu, J., Li, G., Jiang, H. and Zhang, W. (2019), "KNN/PDMS/C-based lead-free piezoelectric composite film for flexible nanogenerator", *J. Mater. Sci. : Mater. Electron*., 1-9. https://doi.org/10.1007/s10854-019-01070-0.

Zhang, G., Li, M., Li, H., Wang, Q. and Jiang, S. (2018), "Harvesting energy from human activity: Ferroelectric energy harvesters for portable, implantable, and biomedical electronics", *Energy Technol.*, **6**(5),791-812. https://doi.org/10.1002/ente.201700622.

HJ